

# Down-regulation of the ATP-binding Cassette Transporter 2 (Abca2) Reduces Amyloid- $\beta$ Production by Altering Nicastrin Maturation and Intracellular Localization\*

Received for publication, August 1, 2011, and in revised form, November 4, 2011. Published, JBC Papers in Press, November 15, 2011, DOI 10.1074/jbc.M111.288258

Vasiliki Michaki<sup>‡§</sup>, Francesc X. Guix<sup>‡§1</sup>, Krist'1 Vennekens<sup>‡§</sup>, Sebastian Munck<sup>‡§</sup>, Colin Dingwall<sup>¶</sup>, John B. Davis<sup>||2</sup>, Danyelle M. Townsend<sup>\*\*</sup>, Kenneth D. Tew<sup>\*\*</sup>, Fabian Feiguin<sup>††</sup>, Bart De Strooper<sup>‡§</sup>, Carlos G. Dotti<sup>‡§§3</sup>, and Tina Wahle<sup>‡4</sup>

From the <sup>‡</sup>Center for Human Genetics and Leuven Institute for Neurodegenerative Diseases (LIND), KU Leuven, 3000 Leuven, Belgium, the <sup>§</sup>Vlaams Instituut voor Biotechnologie, VIB11, 3000 Leuven, Belgium, the <sup>§§</sup>Centro Biología Molecular Severo Ochoa CSIC-UAM, 28049 Madrid, Spain, the <sup>¶</sup>Pharmaceutical Science Division, King's College London, London SE1 9NH, United Kingdom, the <sup>||</sup>Neuroscience Centre of Excellence for Drug Discovery, GlaxoSmithKline R&D Ltd., Harlow CM195AW, United Kingdom, the <sup>\*\*</sup>Department of Pharmaceutical and Biomedical Sciences, Medical University of South Carolina, Charleston, South Carolina 29425, and the <sup>††</sup>International Center for Genetic Engineering and Biotechnology, 34149 Trieste, Italy

**Background:** The intracellular sterol transporter Abca2 has been genetically linked to Alzheimer disease.

**Results:** Abca2 depletion reduces  $\gamma$ -secretase cleavage of APP without affecting  $\gamma$ -cleavage of Notch and alters maturation and intracellular localization of Nicastrin, a member of the  $\gamma$ -secretase complex.

**Conclusion:** Abca2 depletion affects  $\gamma$ -secretase cleavage in a substrate-distinctive manner.

**Significance:** Abca2 is an important regulator of  $\gamma$ -secretase-mediated APP proteolysis and therefore A $\beta$  generation.

Clinical, pharmacological, biochemical, and genetic evidence support the notion that alteration of cholesterol homeostasis strongly predisposes to Alzheimer disease (AD). The ATP-binding cassette transporter-2 (Abca2), which plays a role in intracellular sterol trafficking, has been genetically linked to AD. It is unclear how these two processes are related. Here we demonstrate that down-regulation of Abca2 in mammalian cells leads to decreased amyloid- $\beta$  (A $\beta$ ) generation. *In vitro* studies revealed altered  $\gamma$ -secretase complex formation in Abca2 knock-out cells due to the altered levels, post-translational modification, and subcellular localization of Nicastrin. Reduced Abca2 levels in mammalian cells *in vitro*, in *Drosophila melanogaster* and in mice resulted in altered  $\gamma$ -secretase processing of APP, and thus A $\beta$  generation, without affecting Notch cleavage.

Alzheimer disease (AD)<sup>5</sup> is associated with extracellular deposits of the amyloid  $\beta$ -peptide (A $\beta$ ) and intraneuronal

aggregates of hyperphosphorylated Tau protein in the brain (1). Evidence suggests that the pathogenesis of AD involves deleterious neurotoxic effects of aggregated A $\beta$  peptides (2), which are derived by sequential proteolytic processing of the  $\beta$ -amyloid precursor protein (APP) by  $\beta$ - and  $\gamma$ -secretases. APP can also be cleaved in a nonamyloidogenic pathway that involves initial cleavage by  $\alpha$ -secretase within the A $\beta$  domain that precludes the later generation of A $\beta$  peptides (1, 3, 4). Because the toxicity resulting from excess A $\beta$ , it is of critical importance to understand how these alternative cleavages are regulated. Naturally, because APP and its proteases are all integral membrane proteins, the cleavage of APP will be greatly affected by changes in the lipid content of the cell. Indeed, strong evidence indicates a functional relationship between AD and amyloidogenesis with a lipid metabolism (5–7). In particular, cholesterol is recognized to play a key role in the pathogenesis of AD (8). Many groups have reported that high intracellular cholesterol levels result in enhanced release of A $\beta$  *in vitro* and *in vivo* (9–11), whereas low intracellular cholesterol levels favor processing of APP through the nonamyloidogenic pathway and decrease A $\beta$  production (12, 13). Several studies suggest that the generation of A $\beta$  is highly dependent on the levels of cholesterol within detergent-resistant microdomains (DRMs) of the membrane (14–16). In fact the APP cleaving machinery, namely  $\beta$ - and  $\gamma$ -secretase, has been shown to reside in DRMs (14, 17–19) and its activity depends on membrane cholesterol levels (18, 20, 21). Notably, many of these studies have relied on pharmacological or chemical manipulation of intracellular cholesterol levels, as a result revealing only how APP processing would be affected in certain, extreme, situations. In the physiological scenario, a net-

\* This work was supported in part by the Fund for Scientific Research Flanders (FWO), Federal Office for Scientific Affairs (IUAP P6/43/), Stichting voor Alzheimer Onderzoek/Fondation pour la Recherche sur Maladie d'Alzheimer (SAO/FRMA), the Flemish Government (Methusalem grant), and Spanish Government Grants Ministerio de Ciencia e Innovación Ingenio-Consolider CSD2010-00064 and Ministerio de Ciencia e Innovación SAF2010-14906 (to C. G. D.).

<sup>1</sup> Supported by the Spanish Grant Beatriu de Pinós (AGAUR).

<sup>2</sup> Present address: Convergence Pharmaceuticals Ltd., Cambridge CB22 3AT, UK.

<sup>3</sup> To whom correspondence may be addressed. E-mail: carlos.dotti@med.kuleuven.be.

<sup>4</sup> Supported by European Molecular Biology Organization and Deutsche Forschungsgemeinschaft long-term fellowships. To whom correspondence may be addressed: Laboratory of Neuronal Differentiation, Center for Human Genetics and Leuven Institute for Neurodegenerative diseases (LIND), KU Leuven and Vlaams instituut voor Biotechnologie, VIB11, Herestraat 49-bus 602, 3000 Leuven, Belgium. Tel.: 32-0-16-3-30525; Fax: 32-0-16-3-30939; E-mail: tina.wahle@med.kuleuven.be.

<sup>5</sup> The abbreviations used are: AD, Alzheimer disease; A $\beta$ , amyloid- $\beta$ ; NPC, Niemann-Pick type C; Abca2, ATP-binding cassette transporter-2; APP,

$\beta$ -amyloid precursor protein; DRM, detergent-resistant microdomain; MEF, mouse embryonic fibroblast; BisTris, 2-[bis(2-hydroxyethyl)amino]-2-(hydroxymethyl)propane-1,3-diol; CTF, COOH-terminal fragment; Endo H, endoglycosidase H; PNGase F, N-glycosidase F.

work of genes mediates the regulation of intracellular cholesterol levels and it is likely that variations leading to a late-occurring disease like AD are subtle. This led us to use genetic tools to investigate how cholesterol dyshomeostasis may lead to AD. We focused our attention on the ATP-binding cassette transporter-2 (*Abca2*) for two reasons: (i) *Abca2* has been genetically linked to Alzheimer disease (22, 23) and (ii) *Abca2* plays a role in intracellular sterol trafficking (24).

Abc transporters use ATP hydrolysis to drive the transport of various molecules across biological membranes (25). The human Abc transporters are grouped into seven classes (26), of which *Abca* and *Abcg* classes are believed to act as critical gatekeepers of cholesterol homeostasis (27, 28). *Abca2*, the second identified member of the *Abca* subfamily, is most highly expressed in brain, especially in the white matter (29), and is enriched in pluripotent neural progenitor cells in the subventricular zone of lateral ventricles and dentate gyrus of the hippocampus (30). At the subcellular level, *Abca2* localizes to late endosomes, lysosomes, *trans*-Golgi, and endoplasmic reticulum (31).

Functional studies in CHO cells identified a possible role of *Abca2* in the intracellular trafficking of lipoprotein-derived cholesterol from late endosomes/lysosomes to the endoplasmic reticulum for esterification (32). The endosomal-lysosomal pathway is also known to be the major site of A $\beta$  generation (33–35) and further studies demonstrated a co-localization of *Abca2* and APP in intracellular vesicles of neuroblastoma cells (36). The clinical relevance of *Abca2* is suggested by two independent studies that strongly linked the identical single nucleotide polymorphism to AD (22, 23). However, the underlying molecular mechanism is still unclear.

Here we demonstrate that subcellular *Abca2* levels play an important role in  $\gamma$ -secretase processing of APP and thus in A $\beta$  generation. In mammalian cells, siRNA-mediated knockdown of *Abca2* expression resulted in decreased A $\beta$  generation due to lowered  $\gamma$ -secretase processing of APP. *In vitro*, as well as in *Drosophila melanogaster*, genetic reduction of *Abca2* resulted in decreased  $\gamma$ -secretase-dependent cleavage of APP, whereas Notch processing was not affected. Knockdown of *Abca2* in mammalian cells affected the glycosylation pattern and subcellular localization of Nicastrin leading to altered  $\gamma$ -secretase complex formation. In line with that, *Abca2* knock-out mice displayed reduced Nicastrin protein levels and decreased A $\beta$  generation, whereas Notch processing was unaffected. Taken together our data indicate that *Abca2* is an important regulator of  $\gamma$ -secretase-mediated APP proteolysis and therefore of A $\beta$  generation.

## EXPERIMENTAL PROCEDURES

**Mammalian Cell Lines, Primary Rat Hippocampal Neurons, and Mice**—Human embryonic kidney (HEK) 293 cells stably overexpressing human wild type APP695 or mouse embryonic fibroblast (MEF) cells were grown in Dulbecco's modified Eagle's minimum (DMEM) essential medium (Invitrogen) supplemented with 10% heat-inactivated fetal bovine serum (Perbio) and 100  $\mu$ g/ml of penicillin/streptomycin (Invitrogen). Rat primary hippocampal cultures were prepared from embryonic day 18 brains as previously described (37). For biochemical

analysis  $2 \times 10^5$  cells were plated in 12-well and 3-cm plastic dishes coated with poly-L-lysine (0.1 mg/ml) and containing minimal essential medium with B27 supplement (Invitrogen). Both neurons and cell lines were kept under 5% CO<sub>2</sub> at 37 °C. Generation and maintenance of *Abca2* knock-out mice has been described elsewhere (38).

**Antibodies**—For immunoprecipitation and detection of A $\beta$  and secreted APP $\alpha$  the 6E10 antibody (Covance) was used. APP full-length and APP C-terminal fragments were precipitated with APPCt C-terminal antibody (Sigma). Secreted APP $\beta$  was detected with the specific antibody (39138, Covance). Presenilin was detected with the SB129 antibody, Nicastrin with the 9C3 antibody (39), Aph1a with the B80.3 (40), and Pen2 with anti-Pen2 antibody (40). Actin antibody was purchased from Sigma. For *Abca2* detection, the *Abca2* (N-19) goat polyclonal antibody was used (Santa Cruz Biotechnology). Neuregulin 1 was detected with anti-Nrg1 $\alpha$ / $\beta$ 1/2 (C-20) (Santa Cruz Biotechnology). TGN46 antibody was purchased from BD Biosciences.

**siRNA Design and Transfection**—The siRNA sequences were designed using an RNAi algorithm publicly available. For our assays 100 pmol of siRNA or 4  $\mu$ g of *Abca2* cDNA (38) were transfected per well in a 6-well dish using the transfection reagent Lipofectamine 2000 (Invitrogen), according to the manufacturer's instructions. The shRNA of *Abca2* was cloned in the pLentiLox3.7 vector. 3 Days *in vitro* neurons plated in a 12-well dish were transfected with 1.6  $\mu$ g of the plasmid and Lipofectamine 2000 for 72 h.

**RNA Isolation and Real-time PCR**—The isolation of RNA from cells and brain samples was achieved with the RNeasy Plus kit (Qiagen). cDNA was prepared with the RevertAid First Strand cDNA Synthesis kit from Fermentas, and real-time PCR was performed using the SYBR Green PCR Master Mix assay (Eurogentec) with the ABI PRISM 7000 Sequence Detection System (Applied Biosystems). The quantification was performed against a control housekeeping gene, namely  *$\beta$ -actin*.

**ELISA**—For A $\beta$  peptide detection HEK293 cells were transfected with siRNA and the medium was replaced with fresh medium 48 h post-transfection. Cells were grown for another 24 h and media were assayed for A $\beta$  load using the hA $\beta$ 40 or hA $\beta$ 42 ELISA kit (The Genetics Company) according to the manufacturer's instructions. For rodent A $\beta$  the A $\beta$ 40 ELISA kit from Wako was used.

**Immunoprecipitation and Immunoblotting**—Cells were lysed 72 h post-transfection in STEN lysis buffer (1 $\times$  STEN: 50 mM Tris, pH 7.6, 150 mM NaCl, 2 mM EDTA, 0.2% Nonidet P-40; STEN-lysis buffer, 1% Triton X-100, 1% Nonidet P-40, complete protease inhibitors in 1 $\times$  STEN) and clarified by a 30-min centrifugation at 13,200  $\times$  g. For immunoprecipitation of proteins the lysates or the conditioned media were incubated overnight with the appropriate antibodies and protein G-Sepharose beads (Amersham Biosciences). The beads were washed twice with STEN-NaCl (STEN buffer with 500 mM NaCl), and once with STEN buffer. Upon SDS-PAGE electrophoresis, immunoprecipitated proteins were transferred to nitrocellulose membrane and detected with the corresponding antibodies. Mouse brains were homogenized on ice in RIPA buffer (1% Triton X-100, 1% sodium deoxycholate, 0.1% SDS, 150 mM

## Down-regulation of *Abca2* Reduces A $\beta$ Generation

NaCl, 50 mM Tris-HCl, pH 7.2), using an Ultraturax T25 (Janke & Kunkel). Samples were centrifuged at 15,000  $\times$  g, and supernatants were used for protein determination.

**$\gamma$ -Secretase Luciferase Assay**—HEK293 cells were co-transfected with the UAS-luciferase reporter gene, an APP or Notch reporter construct carrying a Gal4-VP16 (41) in the cytoplasmic domain, and *Abca2* siRNA. After 48 h the cells were lysed and processed according to the manufacturer's instructions (Promega). Emitted light was measured with the microplate reader (Victor3 by PerkinElmer Life Sciences).

***Drosophila* Genetics and Maintenance**—All stocks were maintained at 25 °C and raised on cornmeal-yeast agar medium. The fly reporter C99-GV/UAS-GRIM and hs>C99-GV flies have been previously described (42, 43). The strain Ne511/FM6;Df(N+)/TM2 that was carrying a null allele of Notch was a kind gift of Marco Milan. For the generation of homozygous mutant clones in the eyes, the eyflp system was applied (44). The P-element I(3)S132601/82 from the P(lacW) insertion line (I(3)SXXXXXX) was purchased from the Szeged *Drosophila* Stock Centre. For the genetic screens, virgins from the P-element carrying flies were crossed to males of each reporter stock. Progeny was scored compared with control crossed to the w1118 wild-type flies.

**Blue Native-PAGE**—Cell membranes were prepared as described above and resuspended in buffer containing 0.5% dodecylmaltoside, 20% glycerol, 25 mM BisTris/HCl, pH 7.0, and protease inhibitors, and solubilized for 1 h on ice. After ultracentrifugation (100,000  $\times$  g at 4 °C for 30 and 15 min), the cleared supernatant was collected. For each sample, the same amount was mixed with 5 $\times$  Blue Native sample buffer (2.5% Coomassie Brilliant Blue G-250, 50 mM BisTris/HCl, 250 mM 6-aminocaproic acid, pH 7.0, and 15% sucrose) and stored overnight at 4 °C. Blue Native-PAGE was performed as described previously (45) with some modifications. Samples were loaded on a 5–16% polyacrylamide gel and run at 200 V for 4 h. Before transfer, the gel was treated with transfer buffer containing 0.1% SDS for 10 min.

**Metabolic Labeling**—72 h post-siRNA transfection HEK293 cells stably overexpressing APP695 were starved for 45 min and labeled with radioactive [<sup>35</sup>S]methionine/cysteine for 2 h. Cells were chased for the indicated time points and Nicastrin was immunoprecipitated from the cell lysates. Radiolabeled proteins were visualized with phosphorimaging.

**Immunofluorescence Microscopy**—MEF cells seeded on polylysine-coated coverslips were fixed with 4% paraformaldehyde for 10 min followed by a 1 $\times$  PBS wash and a permeabilization step using 0.01% Triton X-100 in 1 $\times$  PBS for 10 min. After washing twice in 1 $\times$  PBS, cells were blocked and incubated for 1 h at RT with the respective primary antibody diluted in 10% blocking solution. After 5 washes, secondary antibodies also diluted in 10% blocking were incubated for 30 min. Finally, cells were washed and mounted on glass slides.

**Cell Surface Biotinylation**—Cells were washed three times with ice-cold 1 $\times$  PBS and incubated on ice with 1 $\times$  PBS, pH 8, containing 0.5 mg/ml of EZ-link Sulfo-NHS-SS-biotin (Pierce) for 30 min. Cells were then washed three times, 5 min each, with ice-cold 1 $\times$  PBS supplemented with 20 mM glycine and finally washed twice with 1 $\times$  PBS. Cells were lysed as described before.

Biotinylated proteins were immunoprecipitated using streptavidin-agarose. Precipitated Nicastrin was detected by Western blot with 9C3 antibody, and cell surface localization was quantified using ImageJ software.

**Statistical Analysis**—Data are presented as the mean  $\pm$  S.D. *p* values were determined by Student's two-tailed *t* test between control and experimental groups.

## RESULTS

***Abca2* Depletion Decreases A $\beta$  Secretion in Mammalian Cells**—To determine the extent *Abca2* depletion affects the cleavage of APP in mammalian cells, we knocked down *Abca2* by sequence-specific siRNAs in HEK293 cells stably expressing human APP (APP695). siRNA knockdown efficacy was tested after 72 h by measuring *Abca2* mRNA and protein levels in siRNA-treated *versus* nontreated (control) cells (Fig. 1, A and B).

First, we measured A $\beta$  levels in the medium of *Abca2* knocked down cells. ELISA-based analysis of A $\beta$  levels in the medium 72 h post-transfection revealed a significant decrease in A $\beta$ 40, up to 40% (Fig. 1C). Likewise the secretion of A $\beta$ 42 was significantly decreased in *Abca2*-depleted cells compared with controls (up to 30%, Fig. 1C). These results complement recent studies showing that overexpression of *Abca2* leads to increased A $\beta$  production (36, 46). Second, to further validate the positive role of *Abca2* in A $\beta$  generation, we proceeded to analyze the amount of A $\beta$  by peptide immunoprecipitation/Western blot in HEK293 cells stably expressing human APP. The data depicted in Fig. 1D confirm that siRNA knockdown of *Abca2* reduced the amount of secreted A $\beta$ . To give neuronal validity to our experiments, *Abca2* was knocked down in primary rat hippocampal neurons *in vitro*. This also resulted in a significant (20%) decrease in A $\beta$  production (Fig. 1E).

The observation that *Abca2* depletion resulted in reduced A $\beta$  production led us to investigate its effect on activities of the different secretases involved in APP processing. Membrane preparations from nontreated (control) and *Abca2* siRNA-treated HEK293 cells stably overexpressing human APP695 were analyzed for the different APP cleavage products by Western blotting. APP full-length levels were not significantly changed in membrane fractions of *Abca2* siRNA-treated *versus* control cells, indicating that *Abca2* depletion has no direct impact on the expression levels of the precursor protein (Fig. 2A). *Abca2* reduction resulted in increased levels of the APP C-terminal fragments (CTF). Interestingly, compared with cells overexpressing APP alone, cells co-expressing APP and *Abca2* siRNA presented lower levels of CTF $\beta$  and considerably higher levels of CTF $\alpha$  (Fig. 2A). In line with this, knockdown of *Abca2* resulted in the significant decrease of APPs $\beta$  *versus* APPs $\alpha$  in the conditioned media (Fig. 2B), indicating a shift from  $\beta$ - to  $\alpha$ -secretase cleavage of APP. The protein levels of ADAM10, a member of the  $\alpha$ -secretase family, or of  $\beta$ -secretase (BACE1) were not altered (Fig. 2C) suggesting that *Abca2* depletion reduces A $\beta$  generation through the induction of a shift toward the  $\alpha$ -secretase pathway.

To gain further insight into the mechanisms by which *Abca2* reduction leads to decreased A $\beta$  we measured the levels of the intracellular peptide. In HEK293 cells APP is predominantly processed by  $\alpha$ -secretase preventing A $\beta$  generation. To

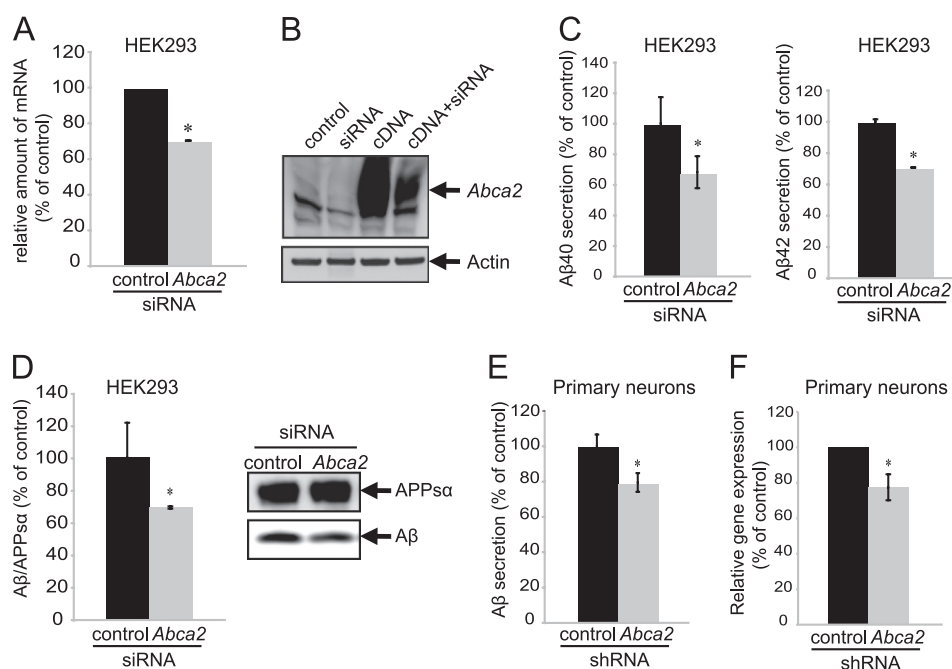


**FIGURE 1. Depletion of Abca2 decreases A $\beta$  secretion in mammalian cells.** HEK293 cells overexpressing APP695 were transfected with siRNA specifically directed against Abca2. *A* and *B*, the efficiency of the siRNA reduction was analyzed 72 h after transfection by quantitative PCR and Western blot. *A*, the graph depicts the relative amount of Abca2 mRNA. *B*, Abca2 protein levels were determined by Western blot. Overexpression of Abca2 in HEK293 cells was used as an additional control for siRNA knock-down efficiency. *C* and *D*, media of HEK293 cells overexpressing APP695 and treated with nontargeting (control) or specific siRNAs against Abca2 were collected 72 h post-transfection. The secreted A $\beta$ 40 and A $\beta$ 42 load was evaluated by ELISA (*C*) and immunoprecipitation of total A $\beta$  with 6E10 antibody (*D*). Quantifications of ELISA and immunoprecipitation are depicted in *panels C* and *D*. Values represent the mean  $\pm$  S.D. of three independent experiments. Significance was determined by Student's *t* test. \*, *p* values are: 0.026 for A $\beta$ 40; 0.00007 for A $\beta$ 42, and 0.017 for total A $\beta$  (IP). Absolute A $\beta$ 40/A $\beta$ 42 levels (pg/ml) of a representative experiment are 195/40 for the control and 137/27 for Abca2 siRNA. *E*, rat hippocampal neurons were transfected with the shRNA against Abca2 cloned in the plentiLox3.7 vector. 72 h later the media were collected and the secreted A $\beta$  was measured by ELISA. A $\beta$ 40 levels (pg/ml) of a representative experiment are: control, 40 and Abca2, 30. Values are presented as means of four assays  $\pm$  S.D. \*, *p* values for Abca2 siRNA-treated cells = 0.008, Student's *t* test. *F*, Abca2 mRNA levels were analyzed by quantitative PCR in primary hippocampal neurons. The graph depicts the relative amount of mRNA normalized to the expression of  $\beta$ -actin. Values are presented as mean  $\pm$  S.D. of three assays. \*, *p* values for Abca2 = 0.03, Student's *t* test.

increase total A $\beta$  levels and determine intracellular A $\beta$  levels HEK293 cells were transiently co-transfected with FLAG-CTF $\beta$  (FLAG-C99) and nontargeting (control) or Abca2-specific siRNAs. Intracellular A $\beta$  levels were measured by peptide immunoprecipitation/Western blot. Intracellular A $\beta$  was found significantly decreased in cells fed with Abca2 siRNA (Fig. 2*D*), indicating that lower levels of A $\beta$  in the media upon knockdown reflect a true effect on peptide generation and not an impaired secretion. In addition, the total amount of CTFs (Fig. 2, *A* and *D*) was increased indicating impaired  $\gamma$ -secretase cleavage or impaired CTF degradation.

**Depletion of Abca2 Decreases  $\gamma$ -Secretase-mediated Cleavage of APP in Vitro and in Vivo**—To determine the impact of Abca2 levels on  $\gamma$ -cleavage of APP we analyzed the levels of AICD production in HEK293 cells expressing APPC99-GAL4/UAS-luciferase reporter constructs. HEK cells were co-transfected with the reporter construct and Abca2 siRNA oligonucleotides; AICD generation was monitored after 72 h. The knockdown of Abca2 resulted in a 30% decrease of AICD generation (Fig. 3*A*).

An important aspect of the  $\gamma$ -secretase activity is substrate promiscuity. The list of proteins processed by the  $\gamma$ -secretase complex is constantly growing yet the one considered most crucial, together with APP, is the Notch receptor. Notch is a type I transmembrane protein, which follows similar sequential proteolysis to that of APP. Cleavage of Notch by the  $\gamma$ -secretase complex leads to the generation of a Notch intracellular cytoplasmic domain, which translocates to the nucleus, where it

acts as a regulator of transcription (47, 48). To investigate the impact of Abca2 levels on  $\gamma$ -cleavage of Notch we used Notch $\Delta$ E-GAL4/UAS-luciferase reporter constructs and the generation of Notch intracellular cytoplasmic domain was determined 72 h post-transfection of the reporter construct with the Abca2 siRNA. In contrast to AICD, generation of the Notch intracellular cytoplasmic domain was not significantly altered (Fig. 3*B*), indicating that Abca2 depletion affects  $\gamma$ -secretase activity in a substrate-specific manner. To assure that depletion of Abca2 does not affect Notch processing in neurons, the expression of the Notch downstream target Hes-1, which is dependent, directly or indirectly, on  $\gamma$ -secretase activity (49) was evaluated in primary rat hippocampal neurons infected with Abca2 shRNA virus. mRNA levels of Hes-1 were not affected by suppression of Abca2, as shown by real-time PCR (Fig. 3*C*), indicating that Abca2 depletion disturbs  $\gamma$ -secretase cleavage with certain substrate selectivity.

To further validate the role of Abca2 in the regulation of  $\gamma$ -cleavage *in vivo* we utilized *D. melanogaster* expressing a chimeric human APP protein comprised of the C99 transmembrane protein fragment of APP fused to the yeast transcription factor GAL4-VP16 (GV), and the cell-death reporter gene GRIM cloned under the GAL4 responsive transcriptional cassette (UAS). In this system, cleavage of C99 causes release of GV that translocates to the nucleus, where it binds UAS and activates expression of GRIM. GRIM triggers what is known as the "rough eye" phenotype, because of the death of the ommatidia.

## Down-regulation of *Abca2* Reduces $A\beta$ Generation

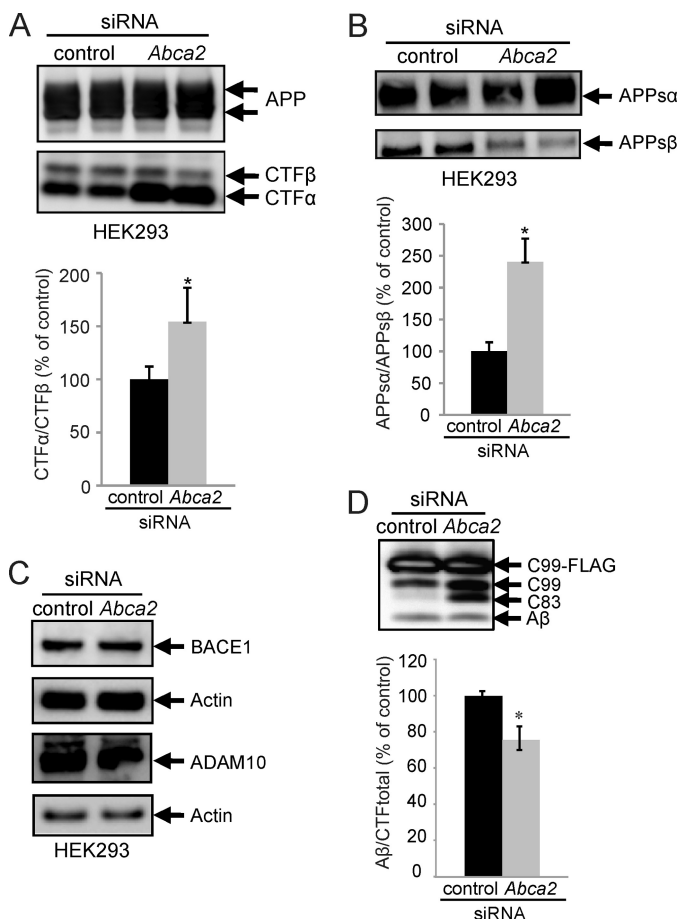


**FIGURE 2. APP processing is affected by *Abca2* reduction.** HEK293 cells expressing APP695 were transfected with nontargeting (*control*) or *Abca2*-specific siRNA. **A** and **B**, 72 h post-transfection the conditioned media was collected and cells were lysed. APP full-length and APP CTFs were detected with APPCt antibody in cellular membrane fractions (**A**). APP is present as a double band corresponding to the mature and immature protein. The graph depicts the CTF $\alpha$ /CTF $\beta$  ratio ( $n = 3$ ; \*,  $p$  values for *Abca2* = 0.003, Student's  $t$  test). **B**, secreted APP $\alpha$  was detected in the conditioned medium with antibody 6E10 that selectively detects APP $\alpha$ , whereas APP $\beta$  was visualized using APP $\beta$ -specific antibody (39138). The graph depicts the APP $\alpha$ /APP $\beta$  ratio ( $n = 3$ ; \*,  $p$  values for *Abca2* < 0.001, Student's  $t$  test). **C**, lysates from HEK293 cells overexpressing APP695 and transfected with the candidate siRNA were analyzed for the expression levels of ADAM10 and BACE1. **D**, in HEK293 cells APP is predominantly processed by  $\alpha$ -secretase preventing A $\beta$  generation. To increase total A $\beta$  levels and determine intracellular A $\beta$  levels HEK293 cells were transiently co-transfected with FLAG-CTF $\beta$  (FLAG-C99) and nontargeting (*control*) or *Abca2*-specific siRNAs. 72 h post-transfection cells were lysed and the intracellular A $\beta$  level was detected by Western blot using 4G8 antibody. Intracellular A $\beta$  levels were normalized against all CTF species (FLAG-C99, endogenous C99 and C83). Note that in *Abca2* knocked down cells all CTF species seem to accumulate. Values represent mean  $\pm$  S.D. of three independent experiments. \*,  $p$  values < 0.01, Student's  $t$  test.

The GMR promoter in front of the C99 leads to the targeting of the GRIM effect only in the eyes. Hereafter, these GMR>C99-GV, UAS-GRIM flies were crossed with the *Abca2* mutant line generated by P-element insertion (33). *Abca2* depletion decreased GRIM expression *in vivo* indicating reduced  $\gamma$ -secretase cleavage of the reporter construct (Fig. 3D). In addition, we used recombinant flies containing the C99-GV construct together with the UAS-GFP reporter gene and a heat shock (*hs*) promoter to induce expression of the C99-GV protein exclusively in adult tissues. For this series of experiments we also took advantage of the eyFLP/FRT technique for targeting

mitotic clones to the eye, which allowed us to generate homozygous mutant clones occupying the eye in flies that also carried the C99-GV, UAS-GFP reporter system in the genetic background (*eyflp*; *hs* > C99-GV, UAS-GFP). These flies were then crossed with the *Abca2* mutant line and progeny bearing homozygous *Abca2* mutant clones in their eyes were collected during 5 days, heat shocked for 1 h at 38 °C, and scored 24 h later for GFP levels. Also in this assay, clear suppression of GFP levels was obtained (Fig. 3E). To determine whether loss of function mutation in the *Abca2* gene was also able to modify the Notch signaling pathway we utilized a hypomorphic allele of Notch called Ne511. This allele shows mild but clear Notch loss of function phenotypes in fly wings among other tissues and, therefore, represents a sensitive genetic background for the Notch pathways. We crossed *Abca2* loss of function flies against the Ne511 allele of Notch and observed that the genetic interactions between these genes did not produce significant differences in wing morphology, compared with wild type controls, indicating that the loss of *Abca2* function most probably does not affect Notch signaling pathways *in vivo* (Fig. 3F). Together, these experiments suggest that *Abca2* depletion affects  $\gamma$ -secretase cleavage of APP in a substrate-specific manner *in vivo*.

***Abca2* Depletion Affects the Levels of  $\gamma$ -Secretase Components *In Vitro* and *In Vivo***—To determine the impact of *Abca2* depletion on the  $\gamma$ -secretase complex, we first investigated the expression levels of the four  $\gamma$ -components, namely Presenilin (PS1), Nicastrin, Pen2, and Aph1. Although the expression of PS1 and Pen2 were unaffected, *Abca2* reduction led to a slight but not significant decrease in the amount of Aph1a (Fig. 4A). Interestingly the mature as well as the immature form of Nicastrin displayed a slightly altered migration pattern, suggesting a change in post-translational modification of the protein. Next, we determined  $\gamma$ -complex formation using Blue Native-PAGE. The exact composition and resolution of the native  $\gamma$ -secretase complex in Blue Native-PAGE has been already described (45). Using this technique we observed a slight shift of mass of the mature  $\gamma$ -complex in *Abca2*-depleted cells (Fig. 4B). To confirm that the observed changes in the  $\gamma$ -complex levels and formation are a true consequence of *Abca2* reduction, we investigated levels of the  $\gamma$ -components as well as formation of the  $\gamma$ -complex in mouse embryonic fibroblasts derived from *Abca2* knock-out mice (38) (Fig. 4, C–E). As in siRNA-treated cells, complete absence of *Abca2* resulted in the electrophoretic migration change of mature and immature Nicastrin (Fig. 4C). Importantly, shift of the mature  $\gamma$ -complex in SDS-PAGE as well as its subcomplexes is more obvious in MEF *Abca2*<sup>-/-</sup> cells than in *Abca2*-depleted HEK293 cells (Fig. 4D). Furthermore, the MEF *Abca2*<sup>-/-</sup> cells showed accumulation of APP CTFs and decreased A $\beta$  secretion (Fig. 4E). As in HEK293 cells the electrophoretic mobility pattern of APP, used as model for the type I transmembrane protein, was not significantly changed in *Abca2*-depleted MEF cells, indicating that *Abca2* plays a role in post-translational modifications (*i.e.* glycosylation or *S*-palmitoylation) of subsets of membrane proteins, among which is Nicastrin.

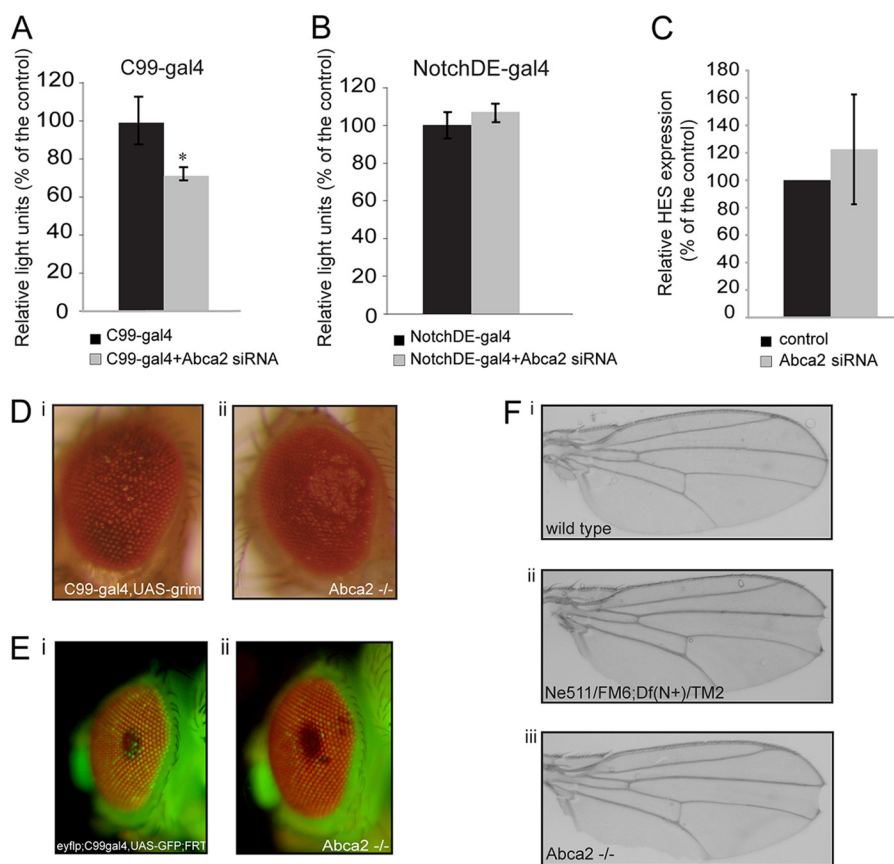


**FIGURE 3. Suppression of *Abca2* modulates  $\gamma$ -cleavage of APP and Notch differently.** *A* and *B*, HEK293 cells were transfected with C99-Gal4-VP16, Notch $\Delta$ E-Gal4-VP16, or Gal4-V16 together with UAS-luciferase (41) and co-transfected with *Abca2* siRNA. The luciferase activities of the  $\gamma$ -secretase-dependent variants were determined: C99-Gal4-VP16 ( $n = 9$ ; \*,  $p < 0.01$ ) and NotchE-Gal4-VP16 ( $n = 6$ ; \*,  $p < 0.05$ ). Values are presented as mean  $\pm$  S.D. and significance was assessed using Student's *t* test. *C*, rat hippocampal neurons were transfected with the shRNAs against *Abca2* cloned in the pLentiLox3.7 vector. Hes-1 mRNA levels were analyzed by quantitative PCR 72 h post-transfection. The graph depicts the relative amount of Hes-1 mRNA normalized to the expression of  $\beta$ -actin. *D–F*, *Drosophila in vivo* read-out systems for  $\gamma$ -secretase cleavage determination. *D*, in APPC99-GV, UAS-GRIM flies  $\gamma$ -secretase cleavage releases the C-terminal part of C99 fused to the Gal4-VP16 sequence, which in turn translocates to the nucleus, binds UAS, and activates GRIM expression, resulting in a rough-eye phenotype (*panel i*). The P-element-induced *Abca2* gene mutation was crossed to the aforementioned reporter stock and progeny were analyzed for suppression or enhancement of the GRIM-induced rough-eye phenotype. As seen in *panel ii*, *Abca2* gene mutation caused a suppression of the phenotype that reflects a suppression of  $\gamma$ -cleavage. *E*, clonal analysis of the effect of the mutation on an inducible read-out system. For the generation of homozygous mutant clones in the eyes, flies that have the heat shock-inducible APPC99-GV/UAS-cd8-GFP reporter system were crossed to *Abca2* mutant flies. The progeny was collected during 5 days, heat shocked for 1 h at 38 °C, and scored 24 h later for levels of GFP expression compared with flies that do not carry the *Abca2* mutation. *F*, evaluation of the effect of *Abca2* depletion on the Notch signaling pathway. *Ne511/FM6;Df(N+)/TM2* flies (*panel ii*) contain a null allele of Notch, which in a heterozygous state produces a dominant phenotype in the wings characterized by nicking the wing margin compared with wild type w1118 flies (*panel i*). To study the effect of the *Abca2* mutation on Notch signaling, *Abca2* mutant flies were crossed to the *Ne511/FM6;Df(N+)/TM2* reporter and progeny wings were examined (*panel iii*).

***Abca2* Depletion Alters Complex Glycosylation and Subcellular Localization of Nicastrin**—To investigate the potential mechanism behind altered  $\gamma$ -complex formation and migration we used *Abca2*-depleted MEF and studied changes in the migration pattern of Nicastrin. After metabolic labeling of the cells, we analyzed the fate of newly formed immature Nicastrin, an  $\sim$ 110-kDa protein that is gradually maturing to a higher molecular mass form. The immature form has a high-mannose oligosaccharide content from its residence in the endoplasmic reticulum. The mature Nicastrin contains a mixed population of endoglycosidase H (Endo H)-sensitive and -resistant oligosaccharides, generated during trafficking through the Golgi apparatus (50). Moreover, Nicastrin can later undergo *S*-palmitoylation (51). Post-translational *S*-palmitoylation is increasingly recognized as a potential mechanism for regulating raft association, stability, intracellular trafficking, and function of several cytosolic and transmembrane proteins (52). Also, *S*-palmitoylation has been shown to contribute

to DRM association of Nicastrin and to be important for its stability (51). Extracts from the metabolically labeled knocked down cells revealed a difference in maturation and migration and a slight decrease in stability of the protein (Fig. 5A). To test if this was due to a change in *S*-palmitoylation *Abca2* siRNA-transfected cells were treated with 2-bromohexadecanoic acid, an inhibitor of palmitoylation. This treatment, however, did not change the migration pattern of Nicastrin (Fig. 5B). In agreement with this, Cheng and colleagues (51) could show that expression of *S*-palmitoylation-deficient Nicastrin in cultured cells does not affect A $\beta$  and AICD production, or intramembrane processing of Notch and N-cadherin. Next, we studied possible changes in the glycosylation pattern of Nicastrin. Nicastrin is synthesized as an endoglycosidase H-sensitive glycosylated precursor protein (immature Nicastrin) and is then modified by complex glycosylation in the Golgi apparatus and by sialylation in the *trans*-Golgi network (mature Nicastrin) (50). Deglycosylation assays using

## Down-regulation of *Abca2* Reduces $A\beta$ Generation

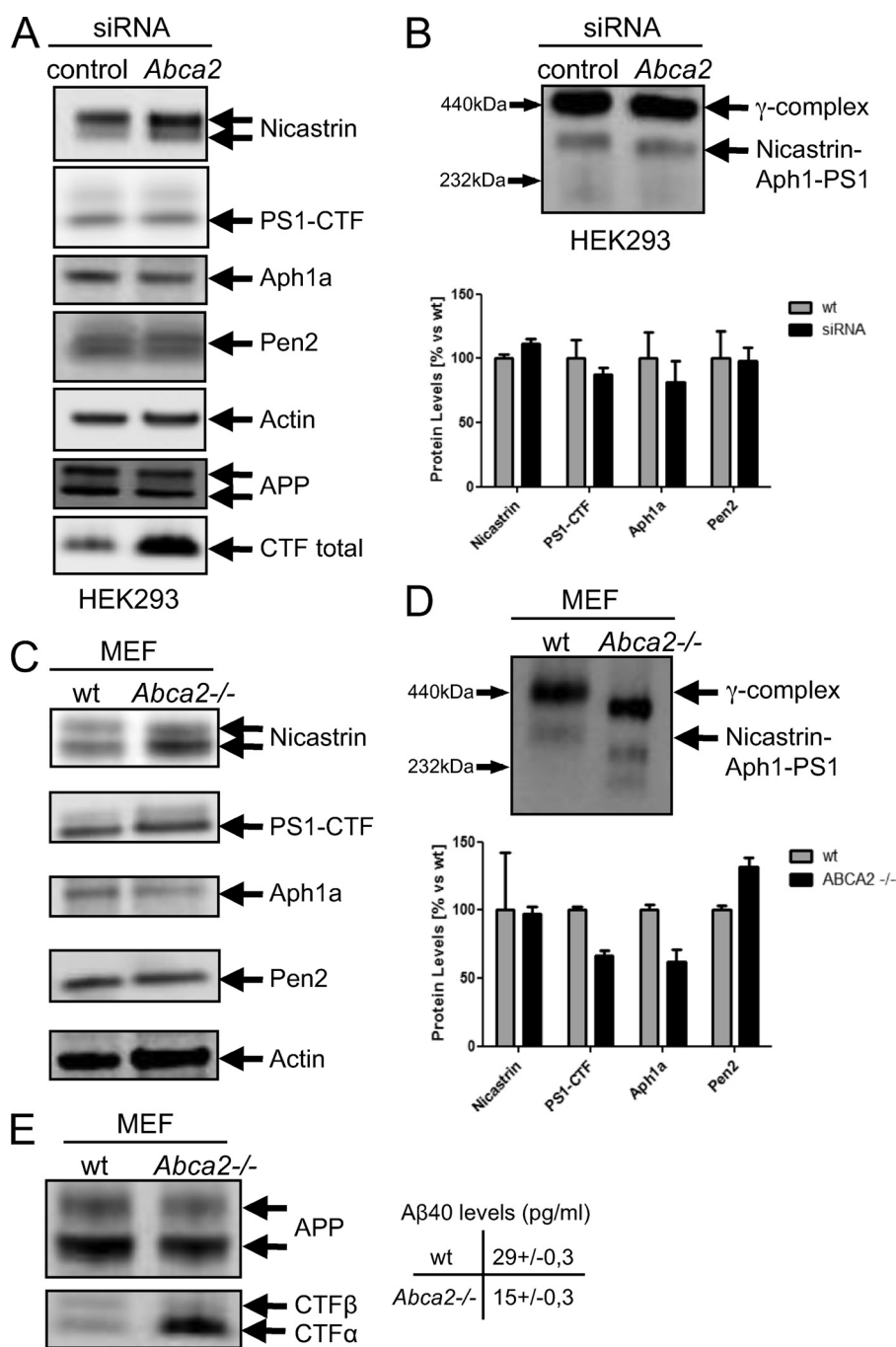


**FIGURE 4. *Abca2* suppression alters  $\gamma$ -complex formation.** *A*, lysates from HEK293 cells overexpressing APP695 and transfected with *Abca2* siRNA were analyzed for expression levels of the components of  $\gamma$ -secretase, namely Presenilin (*PS1-CTF*), Nicastrin, Aph1, and Pen2.  $\beta$ -Actin was used as loading control. Note that Nicastrin appears as a double band corresponding to the mature (*m*) and immature (*im*) protein. The graph depicts the expression levels of the  $\gamma$ -secretase components. *B*, cell membranes of HEK293-APP695 control or *Abca2* siRNA-treated cells were processed for Blue Native-PAGE. Western blot analysis of Nicastrin using 9C3 antibody indicated that down-regulation of *Abca2* results in a shift of the tetrameric mature complexes and the intermediate trimeric (*Nct-Aph1-PS1*) subcomplex. *C*, expression levels of the  $\gamma$ -secretase components were determined in lysates from control or *Abca2*<sup>-/-</sup> depleted MEFs as described above and quantified. *D*, cell membranes of WT or *Abca2*<sup>-/-</sup> MEFs were processed for Blue Native-PAGE. As seen before, depletion of *Abca2* resulted in a shift of the tetrameric mature and intermediate trimeric  $\gamma$ -complexes. *E*, APP full-length and APP CTFs were detected with APPCt antibody in cell membrane fractions of WT and *Abca2*<sup>-/-</sup> MEFs. A $\beta$ 40 levels are depicted in the table. A $\beta$ 42 levels were found to be below the detection limit.

Endo H and PNGase F (*N*-glycosidase F) revealed a distinct migration pattern of the Endo H-resistant form of Nicastrin (Fig. 5C). Endo H digestion reduced the apparent molecular mass of the mature band by ~15 kDa, and the lower band by ~40 kDa. Endo H treatment did not affect the different migration patterns of the mature Nicastrin band in WT and *Abca2*<sup>-/-</sup>-depleted cells. When Nicastrin was treated with PNGase F to remove all

*N*-linked oligosaccharide chains, both proteins co-migrated in SDS-PAGE at the same molecular mass, ~70 kDa, in WT and *Abca2*<sup>-/-</sup> MEF cells. These results indicate that the altered migration of Nicastrin in *Abca2*-depleted cells is due to defective glycosylation.

Because *Abca2* plays a major role in intracellular sterol trafficking (31) the observed effects upon its knockdown may be

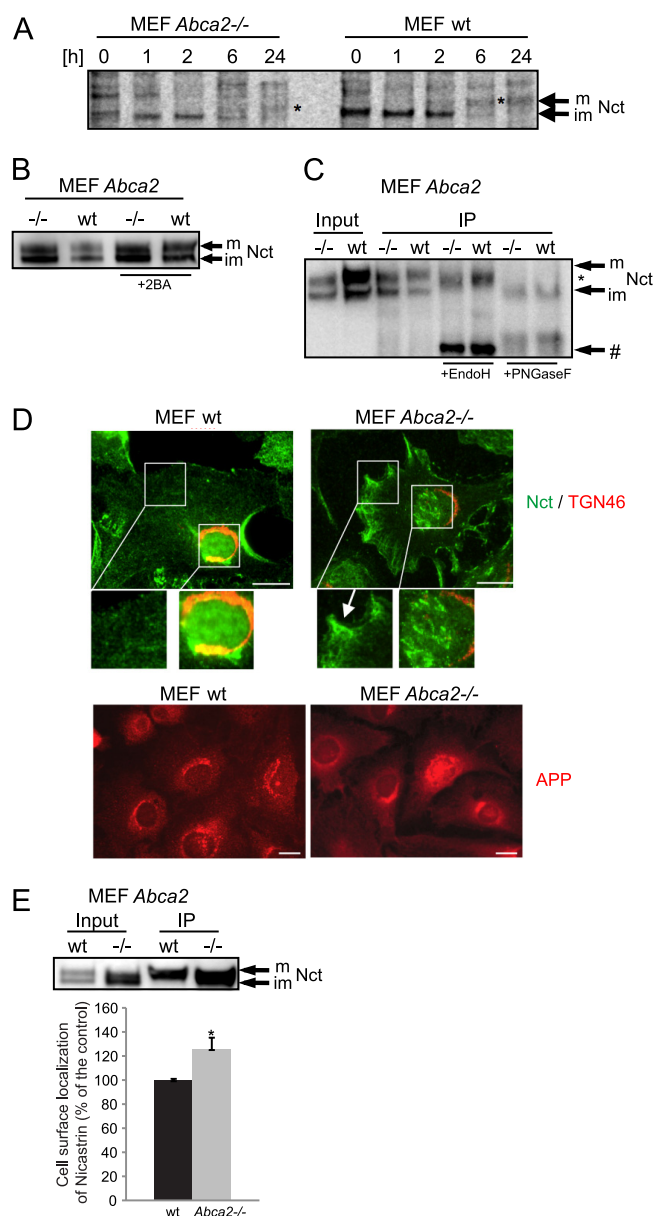


**FIGURE 5. *Abca2* depletion affects the subcellular localization of Nicastrin.** A, control and *Abca2*<sup>-/-</sup> MEFs were pulse labeled with [<sup>35</sup>S]methionine for 15 min. Subsequently, cells were chased for 0–24 h, lysed, and Nicastrin (*Nct*) was immunoprecipitated with 9C3 antibody. Nicastrin appears as a double band corresponding to the (\*) mature (*m*) and immature (*im*) proteins. B, cells were treated with 100  $\mu$ M 2-bromohexadecanoic acid for 16 h to inhibit palmitoylation of the protein. Nicastrin was then detected in membrane fractions. C, deglycosylation assay: Nicastrin was immunoprecipitated with 9C3 and treatment with Endo H or PNGase F was carried out as described under "Experimental Procedures" (left section: total cellular level and right sections: immunoprecipitation (*IP*)). Notice the partial sensitivity of Nicastrin to Endo H (\*) and the complete sensitivity to PNGase F (#). D, the evaluation of the localization immunofluorescence analysis of Nicastrin was performed. Representative images taken for each cell type are shown in the *trans*-Golgi marker TGN46 stained in red and Nicastrin in green. Magnifications depicted below show a representative area of the cell surface as well as the perinuclear region. As can be seen the distribution of Nicastrin (*Nct*) in *Abca2*<sup>-/-</sup> depleted cells is altered, whereas in E, APP localization seems to be unaffected. The scale bar corresponds to 10  $\mu$ m. E, cell surface proteins were labeled with NHS-SS-biotin and isolated with streptavidin-conjugated agarose beads as described under "Experimental Procedures." Precipitates were separated by SDS-PAGE, and Nicastrin (*Nct*) was detected by Western immunoblotting (right sections, *IP*, immunoprecipitation). As a control, cellular levels of these proteins (left section) were visualized. Quantification of Nicastrin cell surface localization of three independent experiments is displayed in the panel below (\*, *p* value = 0.002, Student's *t* test).

the consequence of local changes in cholesterol distribution and defective transport or retention of certain types of proteins in intracellular organelles, depending on their intrinsic requirements to partition in specific lipidic microenvironments. Consistent with this possibility, *Abca2* knockdown resulted in a change in the subcellular distribution of Nicastrin, whereas APP localization did not seem to be affected (Fig. 5D). In fact, rather than concentrated in Golgi, endoplasmic reticulum, and the plasma membrane, Nicastrin appeared in smaller tubules and vesicles in the cell periphery (Fig. 5D). To further examine the altered subcellular localization of Nicastrin we performed cell surface biotinylation experiments. As shown in Fig. 5E, *Abca2* depletion enhanced the cell surface localization of Nicastrin. Interestingly the altered glycosylated band is present at the cell surface (Fig. 5E).

To determine to which extent the observed changes may reflect the *in vivo* situation, A $\beta$  levels were analyzed in brain samples of *Abca2* knock-out mice (38). In these mice, A $\beta$  was decreased, whereas total APP levels were not affected (Fig. 6A). On the other hand, mRNA levels of the Notch downstream target *Hes-1* were not influenced by suppression of *Abca2* (Fig. 6, B and C). Because *Abca2* knock-out mice present altered myelin compaction (38), we also investigated the processing of the  $\gamma$ -secretase substrate Neuregulin 1, which plays a role in myelin sheet formation (53). As described (54, 55), in mouse brain a ~50-kDa band was detected corresponding to the Neuregulin 1 CTF after release of the extracellular domain. We could not detect any significant alteration in the amount of Neuregulin 1 CTF (Fig. 6D) strengthening the view that *Abca2* has substrate selectivity *in vivo*, in the mouse.

As in cells, *Abca2* knock-out mice revealed slightly decreased levels of Aph1a (Fig. 6E). Moreover, *Abca2* depletion led to decreased levels of Nicastrin (Fig. 6E). Unfortunately, the brain lipid composition is not compatible with the biochemical procedures commonly used to detect  $\gamma$ -secretase complex formation (56). Still, we were able to detect a small shift in the electrophoretic mobility of the high molecular weight  $\gamma$ -complexes (Fig. 6F).

## DISCUSSION

***Abca2* Affects Proteolytic Processing of APP**—As a putative cholesterol transporter, *Abca2* has been suggested to contribute to AD by regulating intracellular sterol homeostasis (24). Forced *Abca2* overexpression in Chinese hamster ovary cells showed an accumulation of unesterified low density lipoprotein cholesterol in the endosomal/lysosomal pathway (32), which is involved in proteolytic processing of APP to A $\beta$  (33–35). Sobo and colleagues (57) found that late endosomal accumulation of cholesterol led to impaired intra-endosomal transport and a stabilization of DRMs. DRMs, enriched in cholesterol and sphingolipids, contain active  $\beta$ - and  $\gamma$ -secretase and are known to be principal membrane platforms for amyloidogenic processing of APP (11, 16–18). On the contrary,  $\alpha$ -secretase has been shown to act in non-DRMs (12, 18). As APP at its constitutive levels of expression is mainly restricted to the non-DRMs of neuronal and non-neuronal cells (15, 17), A $\beta$  can only arise by mechanisms that allow the lateral diffusion of the  $\beta$ - and  $\gamma$ -complex away from a DRM or APP toward a DRM. Thus, a



## Down-regulation of *Abca2* Reduces $A\beta$ Generation

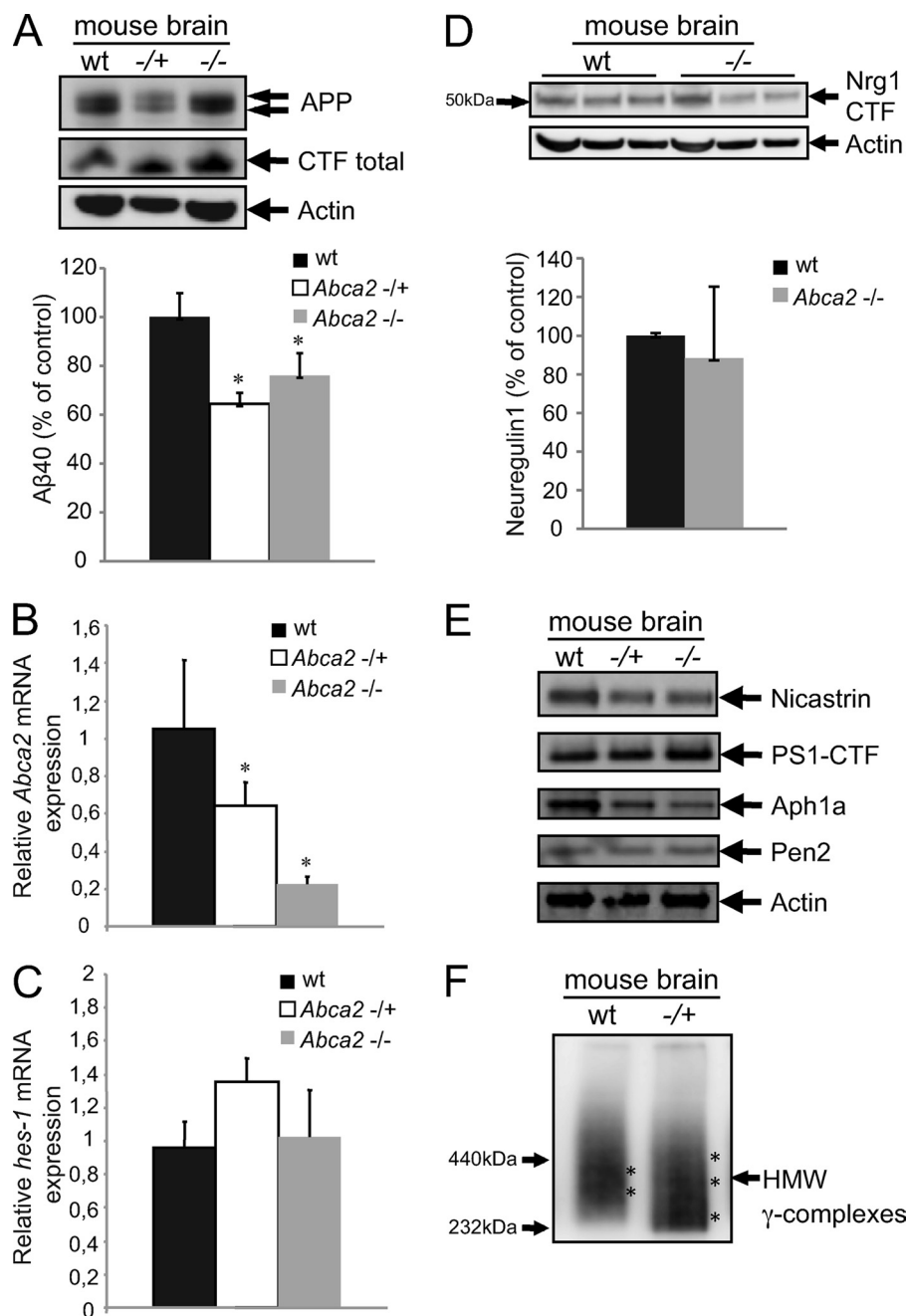


**FIGURE 6. Knockdown of *Abca2* affects the levels of  $\gamma$ -secretase components *in vivo*.** *A*, APP and CTF levels were determined in total brain lysates of 3-month-old *Abca2* WT, heterozygous (-/+), and knock-out (-/-) mice.  $\beta$ -Actin was used as loading control. Endogenous murine  $A\beta_{40}$  levels are depicted in the graph below ( $n = 3$ ; \*,  $p$  value for 0.004 and 0.03, respectively). *B*, the levels of *Abca2* in total brain of *Abca2* WT, heterozygous (-/+), and knock-out (-/-) mice were analyzed by quantitative PCR. The graph illustrates the relative amount of *Abca2* mRNA. *C*, *Hes-1* mRNA levels were analyzed by quantitative PCR in total brain of *Abca2* WT, heterozygous (-/+), and knock-out (-/-) mice. The graph depicts the relative amount of *Hes-1* mRNA normalized to the expression of  $\beta$ -actin. *D*,  $\gamma$ -secretase processing of Neuregulin 1 (*Nrg1*) was analyzed in total brain lysates of *Abca2* WT and knock-out (-/-) mice.  $\beta$ -Actin was used as loading control. *E*, the expression levels of the components of  $\gamma$ -secretase, Presenilin (*PS1-CTF*), Nicastrin, Aph1, and Pen2 were analyzed in total brain lysates of *Abca2* WT, heterozygous (-/+), and knock-out (-/-) mice.  $\beta$ -Actin was used as loading control. It should be noted that in neuronal cells Nicastrin is present as a single band (50). *F*, Blue Native-PAGE analysis of mouse brain samples. Western blot evaluation of Nicastrin using 9C3 indicated that down-regulation of *Abca2* results in a shift of the  $\gamma$ -secretase high molecular weight complexes (HMW) in heterozygous animals (\*, indicates the different migration pattern).

possible explanation for the increased levels of  $\alpha$ -secretase-derived APP cleavage products and concomitant decreased  $\beta$ -secretase processing of APP, is the separation of the cleaving machinery and the substrate APP into distinct membrane microdomains.

Recently, Davis (46) described that *Abca2* overexpression in N2a cells promoted  $\beta$ -secretase cleavage of APP not at the com-

mon Asp1 amino acid site ( $\beta$ -site) of  $A\beta$  but at the Glu<sup>11</sup> site ( $\beta'$ -site) to increase  $\beta'$ -CTF levels.  $\beta'$ -CTF is known to be produced under an excess of  $\beta$ -secretase (58, 59), indicating an enhanced interaction of APP with  $\beta$ -secretase.

In our study we could show that depletion of *Abca2* led to higher  $\alpha$ -secretase cleavage of APP, possibly due to decreased levels and/or altered subcellular distribution of cholesterol. In

fact we observed lower levels of cholesterol in *Abca2*-depleted MEF as well as HEK293 cells (data not shown). This might lead to a modified accessibility of the secretases to APP in microdomains of intracellular organelles or the plasma membrane. Indeed, it has been shown that reducing membrane cholesterol levels through cholesterol-extracting compounds, such as  $\beta$ -methyl cyclodextrin, decreases activity of both BACE1 and  $\gamma$ -secretase, leading to an additive reduction in A $\beta$  generation (13, 60, 61). In line with this, we found decreased  $\gamma$ -secretase cleavage of APP *in vitro* and *in vivo*.

*Abca2 Is a Substrate-selective Modulator of  $\gamma$ -Secretase Activity*—A major finding of this work is the selectivity of *Abca2* on the modulation of APP cleavage. *In vitro* as well as *in vivo* *Abca2* down-regulation did not affect Notch  $\gamma$ -cleavage. Although this cannot be taken as an indicator for absolute substrate specificity, it is still reasonable to describe this molecule as substrate “selective.” Further work is needed to determine the effect on other substrates in the absence of *Abca2*.

An important task for the future is the detailed analysis of the mechanism by which *Abca2* regulates  $\gamma$ -cleavage, particularly in regard to the specificity toward APP. Our data indicate that *Abca2* is a regulator of the secretase-substrate interaction. As depletion of *Abca2* alters at least the intracellular localization of Nicastrin it might lead to a spatial segregation of APP and the  $\gamma$ -secretase complex, whereas the interaction of Notch and the  $\gamma$ -complex remains intact. Although the major site of  $\gamma$ -mediated APP processing is the endosomal-lysosomal system,  $\gamma$ -secretase cleaves Notch also at the plasma membrane (62). In fact in *Abca2*-depleted cells Nicastrin seems to be localized more prominently at the plasma membrane. Again, the spatial segregation occurs not only at the compartmental level but also within microdomains. Intracellular cholesterol also regulates the subcellular distribution of presenilins (10, 63) and inhibition of  $\gamma$ -secretase activity leads to the accumulation of APP CTFs in DRMs (61). By contrast, other  $\gamma$ -secretase substrates, such as Notch 1 and Jagged 2, are largely processed in nonraft compartments (15), once more arguing for the fact that separation of substrate and enzyme is a strong modulator of  $\gamma$ -secretase activity in a substrate-specific manner. It is plausible that the intracellular vesicular localization of *Abca2* may contribute to the accurate distribution of certain components of the A $\beta$  generating machinery.

*Abca2 Depletion Leads to Aberrant Nicastrin Glycosylation and  $\gamma$ -Complex Formation*—*Abca2* depletion *in vitro* as well as *in vivo* led to aberrant maturation of Nicastrin and subsequent aberrant  $\gamma$ -complex formation, a finding not yet described.

Interesting hints for the potential underlying molecular mechanism can be found in the literature. Niemann-Pick type C (NPC) is a rare lipidosis characterized by the accumulation of low density lipoprotein-derived nonesterified cholesterol in the endosomal/lysosomal system and in the *trans*-Golgi network and by consequent disruption of cholesterol homeostasis (64, 65). Both, the NPC1 protein and *Abca2*, co-localize in lysosomal compartments (66) and it has been suggested that these proteins may be functionally antagonistic in regulating the movement of low density lipoprotein-free cholesterol from the late endosomes/lysosomes (32). In fact, *Abca2* overexpression in CHO cells resembles the NPC phenotype and its expression

is elevated in NPC1 fibroblasts (32). Interestingly, NPC1 led to an aberrant glycosylation pattern of NPC2, a small lysosomal protein linked to NPC disease, possibly due to altered deglycosylation of the protein (67). Whether Nicastrin showed a distinct maturation pattern because of defects in deglycosylation in lysosomes or modified glycosylation in the endoplasmic reticulum/Golgi remains to be analyzed. As a matter of fact, it has been shown that small changes in cholesterol content of Golgi membranes specifically inhibit the fusion reaction of the intra-Golgi protein transport. Therefore, cholesterol levels at the Golgi complex must be precisely balanced to allow protein transport (68) and, most likely, proper protein maturation.

In general, protein glycosylation is known to serve several functions including protein folding, stability, trafficking, and protein-protein interaction. Indeed, complex glycosylation of Nicastrin increases its stability (69), its interaction with  $\gamma$ -secretase components, and affects its subcellular localization (70–73). However, *in vitro* inhibition of Nicastrin glycosylation did not affect general  $\gamma$ -secretase activity (50). Still, differences in the levels of mature Nicastrin positively correlated with A $\beta$  secretion, suggesting that proper trafficking and terminal maturation of Nicastrin is a necessary event for the regulated intramembranous proteolysis of APP (74). Actually, immature Nicastrin still appears at the cell surface (50), where  $\gamma$ -secretase could cleave Notch (62). Whether it is the internalization or the trafficking of immature Nicastrin to the endosomal-lysosomal system that is impaired in *Abca2*-depleted cells needs to be determined. In conclusion, this work expands our view on the complexity of  $\gamma$ -secretase assembly and catalysis and how the same enzymatic complex can differentially process diverse substrates.

*Acknowledgments*—We thank Alba Mangas-Losada for technical assistance, Wim Annaert and Jochen Walter and their laboratory members for suggestions and reagents, and Ming Guo for the C99-*Gal4 Drosophila* flies.

## REFERENCES

- Selkoe, D. J. (2001) Alzheimer's disease: genes, proteins, and therapy. *Physiol. Rev.* **81**, 741–766
- Selkoe, D. J. (2008) Biochemistry and molecular biology of amyloid beta-protein and the mechanism of Alzheimer's disease. *Handb. Clin. Neurol.* **89**, 245–260
- Annaert, W., and De Strooper, B. (2002) A cell biological perspective on Alzheimer's disease. *Annu. Rev. Cell Dev. Biol.* **18**, 25–51
- Walter, J., Fluhrer, R., Hartung, B., Willem, M., Kaether, C., Capell, A., Lammich, S., Multhaup, G., and Haass, C. (2001) Phosphorylation regulates intracellular trafficking of beta-secretase. *J. Biol. Chem.* **276**, 14634–14641
- Kalvodova, L., Kahya, N., Schwille, P., Eehalt, R., Verkade, P., Drechsel, D., and Simons, K. (2005) Lipids as modulators of proteolytic activity of BACE: involvement of cholesterol, glycosphingolipids, and anionic phospholipids *in vitro*. *J. Biol. Chem.* **280**, 36815–36823
- Simons, M., Keller, P., Dichgans, J., and Schulz, J. B. (2001) Cholesterol and Alzheimer's disease: is there a link? *Neurology* **57**, 1089–1093
- Vetrivel, K. S., and Thinakaran, G. (2006) Amyloidogenic processing of beta-amyloid precursor protein in intracellular compartments. *Neurology* **66**, S69–73
- Wolozin, B. (2004) Cholesterol and the biology of Alzheimer's disease. *Neuron* **41**, 7–10
- Refolo, L. M., Malester, B., LaFrancois, J., Bryant-Thomas, T., Wang, R.,

## Down-regulation of *Abca2* Reduces A $\beta$ Generation

- Tint, G. S., Sambamurti, K., Duff, K., and Pappolla, M. A. (2000) Hypercholesterolemia accelerates the Alzheimer's amyloid pathology in a transgenic mouse model. *Neurobiol. Dis.* **7**, 321–331
- Burns, M., Gaynor, K., Olm, V., Mercken, M., LaFrancois, J., Wang, L., Mathews, P. M., Noble, W., Matsuoka, Y., and Duff, K. (2003) Presenilin redistribution associated with aberrant cholesterol transport enhances beta-amyloid production in vivo. *J. Neurosci.* **23**, 5645–5649
  - Wahrle, S., Das, P., Nyborg, A. C., McLendon, C., Shoji, M., Kawarabayashi, T., Younkin, L. H., Younkin, S. G., and Golde, T. E. (2002) Cholesterol-dependent gamma-secretase activity in buoyant cholesterol-rich membrane microdomains. *Neurobiol. Dis.* **9**, 11–23
  - Kojro, E., Gimpl, G., Lammich, S., Marz, W., and Fahrenholz, F. (2001) Low cholesterol stimulates the nonamyloidogenic pathway by its effect on the alpha-secretase ADAM 10. *Proc. Natl. Acad. Sci. U.S.A.* **98**, 5815–5820
  - Simons, M., Keller, P., De Strooper, B., Beyreuther, K., Dotti, C. G., and Simons, K. (1998) Cholesterol depletion inhibits the generation of beta-amyloid in hippocampal neurons. *Proc. Natl. Acad. Sci. U.S.A.* **95**, 6460–6464
  - Cordy, J. M., Hussain, I., Dingwall, C., Hooper, N. M., and Turner, A. J. (2003) Exclusively targeting beta-secretase to lipid rafts by GPI-anchor addition up-regulates beta-site processing of the amyloid precursor protein. *Proc. Natl. Acad. Sci. U.S.A.* **100**, 11735–11740
  - Vetrivel, K. S., Cheng, H., Kim, S. H., Chen, Y., Barnes, N. Y., Parent, A. T., Sisodia, S. S., and Thinakaran, G. (2005) Spatial segregation of gamma-secretase and substrates in distinct membrane domains. *J. Biol. Chem.* **280**, 25892–25900
  - Vetrivel, K. S., Cheng, H., Lin, W., Sakurai, T., Li, T., Nukina, N., Wong, P. C., Xu, H., and Thinakaran, G. (2004) Association of gamma-secretase with lipid rafts in post-Golgi and endosome membranes. *J. Biol. Chem.* **279**, 44945–44954
  - Abad-Rodriguez, J., Ledesma, M. D., Craessaerts, K., Perga, S., Medina, M., Delacourte, A., Dingwall, C., De Strooper, B., and Dotti, C. G. (2004) Neuronal membrane cholesterol loss enhances amyloid peptide generation. *J. Cell Biol.* **167**, 953–960
  - Ehehalt, R., Keller, P., Haass, C., Thiele, C., and Simons, K. (2003) Amyloidogenic processing of the Alzheimer beta-amyloid precursor protein depends on lipid rafts. *J. Cell Biol.* **160**, 113–123
  - Riddell, D. R., Christie, G., Hussain, I., and Dingwall, C. (2001) Compartmentalization of beta-secretase (Asp2) into low-buoyant density, non-caveolar lipid rafts. *Curr. Biol.* **11**, 1288–1293
  - Grimm, M. O., Grimm, H. S., Tomic, I., Beyreuther, K., Hartmann, T., and Bergmann, C. (2008) Independent inhibition of Alzheimer disease beta- and gamma-secretase cleavage by lowered cholesterol levels. *J. Biol. Chem.* **283**, 11302–11311
  - Xiong, H., Callaghan, D., Jones, A., Walker, D. G., Lue, L. F., Beach, T. G., Sue, L. I., Woulfe, J., Xu, H., Stanimirovic, D. B., and Zhang, W. (2008) Cholesterol retention in Alzheimer's brain is responsible for high beta- and gamma-secretase activities and A $\beta$  production. *Neurobiol. Dis.* **29**, 422–437
  - Macé, S., Cousin, E., Ricard, S., Génin, E., Spanakis, E., Lafargue-Soubigou, C., Génin, B., Fournel, R., Roche, S., Haussy, G., Massey, F., Soubigou, S., Bréfort, G., Benoit, P., Brice, A., Campion, D., Hollis, M., Pradier, L., Benavides, J., and Deleuze, J. F. (2005) ABCA2 is a strong genetic risk factor for early-onset Alzheimer's disease. *Neurobiol. Dis.* **18**, 119–125
  - Wollmer, M. A., Kapaki, E., Hersberger, M., Muntwyler, J., Brunner, F., Tsolaki, M., Akatsu, H., Kosaka, K., Michikawa, M., Molyva, D., Parakevas, G. P., Lutjohann, D., von Eckardstein, A., Hock, C., Nitsch, R. M., and Papassotiropoulos, A. (2006) Ethnicity-dependent genetic association of ABCA2 with sporadic Alzheimer's disease. *Am. J. Med. Genet. B Neuropsychiatr. Genet.* **141B**, 534–536
  - Mack, J. T., Brown, C. B., and Tew, K. D. (2008) ABCA2 as a therapeutic target in cancer and nervous system disorders. *Expert Opin. Ther. Targets* **12**, 491–504
  - Higgins, J. J., Patterson, M. C., Dambrosia, J. M., Pikus, A. T., Pentchev, P. G., Sato, S., Brady, R. O., and Barton, N. W. (1992) A clinical staging classification for type C Niemann-Pick disease. *Neurology* **42**, 2286–2290
  - Klein, I., Sarkadi, B., and Váradi, A. (1999) An inventory of the human ABC proteins. *Biochim. Biophys. Acta* **1461**, 237–262
  - Schmitz, G., and Kaminski, W. E. (2001) ABC transporters and cholesterol metabolism. *Front. Biosci.* **6**, D505–514
  - Dean, M., Hamon, Y., and Chimini, G. (2001) The human ATP-binding cassette (ABC) transporter superfamily. *J. Lipid Res.* **42**, 1007–1017
  - Zhao, L. X., Zhou, C. J., Tanaka, A., Nakata, M., Hirabayashi, T., Amachi, T., Shioda, S., Ueda, K., and Inagaki, N. (2000) Cloning, characterization and tissue distribution of the rat ATP-binding cassette (ABC) transporter ABC2/ABCA2. *Biochem. J.* **350**, 865–872
  - Broccardo, C., Nieoullon, V., Amin, R., Masméjean, F., Carta, S., Tassi, S., Pophillat, M., Rubartelli, A., Pierres, M., Rougon, G., Nieoullon, A., Chazal, G., and Chimini, G. (2006) ABCA2 is a marker of neural progenitors and neuronal subsets in the adult rodent brain. *J. Neurochem.* **97**, 345–355
  - Mack, J. T., Townsend, D. M., Beljanski, V., and Tew, K. D. (2007) The ABCA2 transporter: intracellular roles in trafficking and metabolism of LDL-derived cholesterol and sterol-related compounds. *Curr. Drug Metab.* **8**, 47–57
  - Davis, W., Jr., Boyd, J. T., Ile, K. E., and Tew, K. D. (2004) Human ATP-binding cassette transporter-2 (ABCA2) positively regulates low-density lipoprotein receptor expression and negatively regulates cholesterol esterification in Chinese hamster ovary cells. *Biochim. Biophys. Acta* **1683**, 89–100
  - Rouyer, O., Talha, S., Di Marco, P., Ellero, B., Doutreleau, S., Diemunsch, P., Piquard, F., and Geny, B. (2009) Lack of endothelial dysfunction in patients under tacrolimus after orthotopic liver transplantation. *Clin. Transplant.* **23**, 897–903
  - Thaveau, F., Zoll, J., Bouitbir, J., Ribera, F., Di Marco, P., Chakfe, N., Kretz, J. G., Piquard, F., and Geny, B. (2009) Contralateral leg as a control during skeletal muscle ischemia-reperfusion. *J. Surg. Res.* **155**, 65–69
  - Grbovic, O. M., Mathews, P. M., Jiang, Y., Schmidt, S. D., Dinakar, R., Summers-Terio, N. B., Ceresa, B. P., Nixon, R. A., and Cataldo, A. M. (2003) Rab5-stimulated up-regulation of the endocytic pathway increases intracellular beta-cleaved amyloid precursor protein carboxyl-terminal fragment levels and A $\beta$  production. *J. Biol. Chem.* **278**, 31261–31268
  - Chen, Z. J., Vulevic, B., Ile, K. E., Soulika, A., Davis, W., Jr., Reiner, P. B., Connop, B. P., Nathwani, P., Trojanowski, J. Q., and Tew, K. D. (2004) Association of ABCA2 expression with determinants of Alzheimer's disease. *FASEB J.* **18**, 1129–1131
  - Kaech, S., and Banker, G. (2006) Culturing hippocampal neurons. *Nat. Protoc.* **1**, 2406–2415
  - Mack, J. T., Beljanski, V., Soulika, A. M., Townsend, D. M., Brown, C. B., Davis, W., and Tew, K. D. (2007) "Skittish" *Abca2* knockout mice display tremor, hyperactivity, and abnormal myelin ultrastructure in the central nervous system. *Mol. Cell Biol.* **27**, 44–53
  - Esselens, C., Oorschot, V., Baert, V., Raemaekers, T., Spittaels, K., Sernaeels, L., Zheng, H., Saftig, P., De Strooper, B., Klumperman, J., and Annaert, W. (2004) Presenilin 1 mediates the turnover of telencephalin in hippocampal neurons via an autophagic degradative pathway. *J. Cell Biol.* **166**, 1041–1054
  - Nyabi, O., Bentahir, M., Horr, K., Herremans, A., Gottardi-Littell, N., Van Broeckhoven, C., Merchiers, P., Spittaels, K., Annaert, W., and De Strooper, B. (2003) Presenilins mutated at Asp-257 or Asp-385 restore Pen-2 expression and Nicastrin glycosylation but remain catalytically inactive in the absence of wild type Presenilin. *J. Biol. Chem.* **278**, 43430–43436
  - Serneels, L., Dejaegere, T., Craessaerts, K., Horr, K., Jorissen, E., Tousseyn, T., Hébert, S., Coolen, M., Martens, G., Zwijsen, A., Annaert, W., Hartmann, D., and De Strooper, B. (2005) Differential contribution of the three *Aph1* genes to gamma-secretase activity in vivo. *Proc. Natl. Acad. Sci. U.S.A.* **102**, 1719–1724
  - Struhl, G., and Adachi, A. (2000) Requirements for presenilin-dependent cleavage of notch and other transmembrane proteins. *Mol. Cell Biol.* **6**, 625–636
  - Guo, M., Hong, E. J., Fernandes, J., Zipursky, S. L., and Hay, B. A. (2003) A reporter for amyloid precursor protein gamma-secretase activity in *Drosophila*. *Hum. Mol. Genet.* **12**, 2669–2678
  - Newsome, T. P., Asling, B., and Dickson, B. J. (2000) Analysis of *Drosophila* photoreceptor axon guidance in eye-specific mosaics. *Development* **127**, 851–860

45. Bammens, L., Chávez-Gutierrez, L., Tolia, A., Zwijsen, A., and De Strooper, B. (2011) Functional and topological analysis of Pen-2, the fourth subunit of the gamma-secretase complex. *J. Biol. Chem.* **286**, 12271–12282
46. Davis, W., Jr. (2010) The ATP-binding cassette transporter-2 (ABCA2) increases endogenous amyloid precursor protein expression and Abeta fragment generation. *Curr. Alzheimer Res.* **7**, 566–577
47. De Strooper, B., Annaert, W., Cupers, P., Saftig, P., Craessaerts, K., Mumm, J. S., Schroeter, E. H., Schrijvers, V., Wolfe, M. S., Ray, W. J., Goate, A., and Kopan, R. (1999) A presenilin-1-dependent gamma-secretase-like protease mediates release of Notch intracellular domain. *Nature* **398**, 518–522
48. Struhl, G., and Greenwald, I. (1999) Presenilin is required for activity and nuclear access of Notch in *Drosophila*. *Nature* **398**, 522–525
49. Louvi, A., and Artavanis-Tsakonas, S. (2006) Notch signalling in vertebrate neural development. *Nat. Rev. Neurosci.* **7**, 93–102
50. Herreman, A., Van Gassen, G., Bentahir, M., Nyabi, O., Craessaerts, K., Mueller, U., Annaert, W., and De Strooper, B. (2003) gamma-Secretase activity requires the presenilin-dependent trafficking of nicastrin through the Golgi apparatus but not its complex glycosylation. *J. Cell Sci.* **116**, 1127–1136
51. Cheng, H., Vetrivel, K. S., Drisdell, R. C., Meckler, X., Gong, P., Leem, J. Y., Li, T., Carter, M., Chen, Y., Nguyen, P., Iwatsubo, T., Tomita, T., Wong, P. C., Green, W. N., Kounnas, M. Z., and Thinakaran, G. (2009) S-palmitoylation of gamma-secretase subunits nicastrin and APH-1. *J. Biol. Chem.* **284**, 1373–1384
52. Linder, M. E., and Deschenes, R. J. (2007) Palmitoylation: policing protein stability and traffic. *Nat. Rev. Mol. Cell Biol.* **8**, 74–84
53. Michailov, G. V., Sereda, M. W., Brinkmann, B. G., Fischer, T. M., Haug, B., Birchmeier, C., Role, L., Lai, C., Schwab, M. H., and Nave, K. A. (2004) Axonal neuregulin-1 regulates myelin sheath thickness. *Science* **304**, 700–703
54. DeJaegere, T., Serneels, L., Schäfer, M. K., Van Biervliet, J., Horré, K., Depboylu, C., Alvarez-Fischer, D., Herreman, A., Willem, M., Haass, C., Höglinger, G. U., D'Hooge, R., and De Strooper, B. (2008) Deficiency of Aph1B/C-gamma-secretase disturbs Nrg1 cleavage and sensorimotor gating that can be reversed with antipsychotic treatment. *Proc. Natl. Acad. Sci. U.S.A.* **105**, 9775–9780
55. Falls, D. L. (2003) Neuregulins and the neuromuscular system: 10 years of answers and questions. *J. Neurocytol.* **32**, 619–647
56. Culvenor, J. G., Ilaya, N. T., Ryan, M. T., Canterford, L., Hoke, D. E., Williamson, N. A., McLean, C. A., Masters, C. L., and Evin, G. (2004) Characterization of presenilin complexes from mouse and human brain using Blue Native gel electrophoresis reveals high expression in embryonic brain and minimal change in complex mobility with pathogenic presenilin mutations. *Eur. J. Biochem.* **271**, 375–385
57. Sobo, K., Le Blanc, I., Luyet, P. P., Fivaz, M., Ferguson, C., Parton, R. G., Gruenberg, J., and van der Goot, F. G. (2007) Late endosomal cholesterol accumulation leads to impaired intra-endosomal trafficking. *PLoS One* **2**, e851
58. Liu, K., Doms, R. W., and Lee, V. M. (2002) Glu11 site cleavage and N-terminally truncated A beta production upon BACE overexpression. *Biochemistry* **41**, 3128–3136
59. Fluhner, R., Capell, A., Westmeyer, G., Willem, M., Hartung, B., Condron, M. M., Teplow, D. B., Haass, C., and Walter, J. (2002) A non-amyloidogenic function of BACE-2 in the secretory pathway. *J. Neurochem.* **81**, 1011–1020
60. Hartmann, T. (2006) Role of amyloid precursor protein, amyloid-beta and gamma-secretase in cholesterol maintenance. *Neurodegener. Dis.* **3**, 305–311
61. Vetrivel, K. S., and Thinakaran, G. (2010) Membrane rafts in Alzheimer's disease beta-amyloid production. *Biochim. Biophys. Acta* **1801**, 860–867
62. Sorensen, E. B., and Conner, S. D. (2010)  $\gamma$ -Secretase-dependent cleavage initiates notch signaling from the plasma membrane. *Traffic* **11**, 1234–1245
63. Runz, H., Rietdorf, J., Tomic, I., de Bernard, M., Beyreuther, K., Pepperkok, R., and Hartmann, T. (2002) Inhibition of intracellular cholesterol transport alters presenilin localization and amyloid precursor protein processing in neuronal cells. *J. Neurosci.* **22**, 1679–1689
64. Pentchev, P. G., Brady, R. O., Blanchette-Mackie, E. J., Vanier, M. T., Carstea, E. D., Parker, C. C., Goldin, E., and Roff, C. F. (1994) The Niemann-Pick C lesion and its relationship to the intracellular distribution and utilization of LDL cholesterol. *Biochim. Biophys. Acta* **1225**, 235–243
65. Vanier, M. T., Rodriguez-Lafrasse, C., Rousson, R., Gazzah, N., Juge, M. C., Pentchev, P. G., Revol, A., and Louisot, P. (1991) Type C Niemann-Pick disease: spectrum of phenotypic variation in disruption of intracellular LDL-derived cholesterol processing. *Biochim. Biophys. Acta* **1096**, 328–337
66. Neufeld, E. B., Wastney, M., Patel, S., Suresh, S., Cooney, A. M., Dwyer, N. K., Roff, C. F., Ohno, K., Morris, J. A., Carstea, E. D., Incardona, J. P., Strauss, J. F., 3rd, Vanier, M. T., Patterson, M. C., Brady, R. O., Pentchev, P. G., and Blanchette-Mackie, E. J. (1999) The Niemann-Pick C1 protein resides in a vesicular compartment linked to retrograde transport of multiple lysosomal cargo. *J. Biol. Chem.* **274**, 9627–9635
67. Chen, F. W., Gordon, R. E., and Ioannou, Y. A. (2005) NPC1 late endosomes contain elevated levels of non-esterified ("free") fatty acids and an abnormally glycosylated form of the NPC2 protein. *Biochem. J.* **390**, 549–561
68. Stüven, E., Porat, A., Shimron, F., Fass, E., Kaloyanova, D., Brügger, B., Wieland, F. T., Elazar, Z., and Helms, J. B. (2003) Intra-Golgi protein transport depends on a cholesterol balance in the lipid membrane. *J. Biol. Chem.* **278**, 53112–53122
69. Tomita, T., Katayama, R., Takikawa, R., and Iwatsubo, T. (2002) Complex N-glycosylated form of nicastrin is stabilized and selectively bound to presenilin fragments. *FEBS Lett.* **520**, 117–121
70. Gu, Y., Chen, F., Sanjo, N., Kawarai, T., Hasegawa, H., Duthie, M., Li, W., Ruan, X., Luthra, A., Mount, H. T., Tandon, A., Fraser, P. E., and St George-Hyslop, P. (2003) APH-1 interacts with mature and immature forms of presenilins and nicastrin and may play a role in maturation of presenilin-nicastrin complexes. *J. Biol. Chem.* **278**, 7374–7380
71. Kimberly, W. T., LaVoie, M. J., Ostaszewski, B. L., Ye, W., Wolfe, M. S., and Selkoe, D. J. (2002) Complex N-linked glycosylated nicastrin associates with active gamma-secretase and undergoes tight cellular regulation. *J. Biol. Chem.* **277**, 35113–35117
72. Edbauer, D., Winkler, E., Haass, C., and Steiner, H. (2002) Presenilin and nicastrin regulate each other and determine amyloid beta-peptide production via complex formation. *Proc. Natl. Acad. Sci. U.S.A.* **99**, 8666–8671
73. Yang, D. S., Tandon, A., Chen, F., Yu, G., Yu, H., Arawaka, S., Hasegawa, H., Duthie, M., Schmidt, S. D., Ramabhadran, T. V., Nixon, R. A., Mathews, P. M., Gandy, S. E., Mount, H. T., St George-Hyslop, P., and Fraser, P. E. (2002) Mature glycosylation and trafficking of nicastrin modulate its binding to presenilins. *J. Biol. Chem.* **277**, 28135–28142
74. Arawaka, S., Hasegawa, H., Tandon, A., Janus, C., Chen, F., Yu, G., Kikuchi, K., Koyama, S., Kato, T., Fraser, P. E., and St. George-Hyslop, P. (2002) The levels of mature glycosylated nicastrin are regulated and correlate with gamma-secretase processing of amyloid beta-precursor protein. *J. Neurochem.* **83**, 1065–1071